ELSEVIER

Journal of Photochemistry and Photobiology A: Chemistry 122 (1999) 151–159

Journal of Photochemistry and Photobiology A:Chemistry

Nodal-plane model of the excited-state intramolecular proton transfer of 2-(*o*-hydroxyaryl)benzazoles

Shin-ichi Nagaoka[a,*], Jyunya Kusunoki[a], Tonan Fujibuchi[a], Seiji Hatakenaka[a], Kazuo Mukai[a], Umpei Nagashima[b]

[a]*Department of Chemistry, Faculty of Science, Ehime University, Matsuyama 790-8577, Japan*
[b]*National Institute of Materials and Chemical Research, Agency of Industrial Science and Technology, Ministry of International Trade and Industry, 1-1 Higashi, Tsukuba, Ibaraki 305-8565, Japan*

Received 13 November 1998; received in revised form 22 January 1999; accepted 27 January 1999

Abstract

The excited-state intramolecular proton transfer of 2-(*o*-hydroxyaryl)benzazoles has been studied by emission spectroscopy. Although both 2-(2-hydroxy-3-aryl)benzazole and 2-(1-hydroxy-2-aryl)benzazole consist of an aryl moiety, a benzazol-2-yl group and an OH group, their emission properties are very different for the reasons that can be explained in terms of our previously offered nodal-plane model.

Keywords: Excited state intramolecular proton transfer; 2-(*o*-Hydroxyaryl)benzazoles; Nodal-plane model

1. Introduction

Much attention has been directed from both experimental and theoretical viewpoints to the excited state intramolecular proton transfer (ESIPT) of hydrogen-bonded molecules [1–10]. ESIPT is a very simple chemical process readily accessible for both accurate measurement and quantitative theoretical analysis. The study of ESIPT is at the forefront of the revolution in the understanding of chemical reactions at the molecular level. It also plays an important role both in fundamental biochemistry and in practical application: the ESIPT of hypericin and related molecules is of current interest because of the anti-viral (especially anti-human-immunodeficiency virus (HIV)) and the anti-tumor activities of these molecules [11]. A molecule showing ESIPT will also be useful in future optical memories and switches [12–14]. Furthermore, ESIPT is also of great interest in view of its relevance to fluorescence probes for biomolecules [15,16], to UV absorbers for polymers [17] and cosmetics [18], to proton transfer laser-dye [19] and to radiation detection scintillators [20].

We have investigated the dynamic processes in the low-lying excited states of *o*-hydroxybenzaldehyde (OHBA) and its related molecules (OHBAs) by using spectroscopic and computational methods [21–36]. We have constructed a simple theoretical model of the ESIPT of OHBAs based on the nodal pattern of the wave function [25,26]. Although this nodal-plane model is a qualitative one, it allows us to recognize the important features of ESIPT immediately and provides useful information about the reaction mechanisms. Our nodal-plane model is applicable to photochemical reactions in various excited states of various molecules [37,38]. Many chemists have cited it [5,8,10,39–49], and the usefulness of our explanation is recognized by many researchers [5,8,39–41,44,48,49].

In this article, we discuss the application of our nodal-plane model to the ESIPT of the 2-(*o*-hydroxyaryl)benzazoles (2-(*o*-hydroxynaphtyl)benzazoles and 2-(*o*-hydroxyanthryl)benzothiazoles) whose structures are shown in Fig. 1. Although the ESIPT of 2-(*o*-hydroxynaphtyl)benzazoles was studied previously [50–56], the dependence of ESIPT on the structure of the isomers (Fig. 1) has not yet been investigated. Section 2 briefly summarizes the understanding of ESIPT by using our nodal-plane model. Section 3 describes experiments with 2-(*o*-hydroxyaryl)-benzazoles and notes that the results of those experiments are consistent with our nodal-plane model. The last section summarizes our conclusions. The work reported in this paper was presented at the 17th IUPAC Symposium on Photochemistry [57].

*Corresponding author. Present address. Institute for Molecular Science, Okazaki 444-8585, Japan. Tel.: +81-564-55-7441; fax: +81-564-54-2254; e-mail: nagaoka@ims.ac.jp

1010-6030/99/$ – see front matter
PII: S1010-6030(99)00025-8

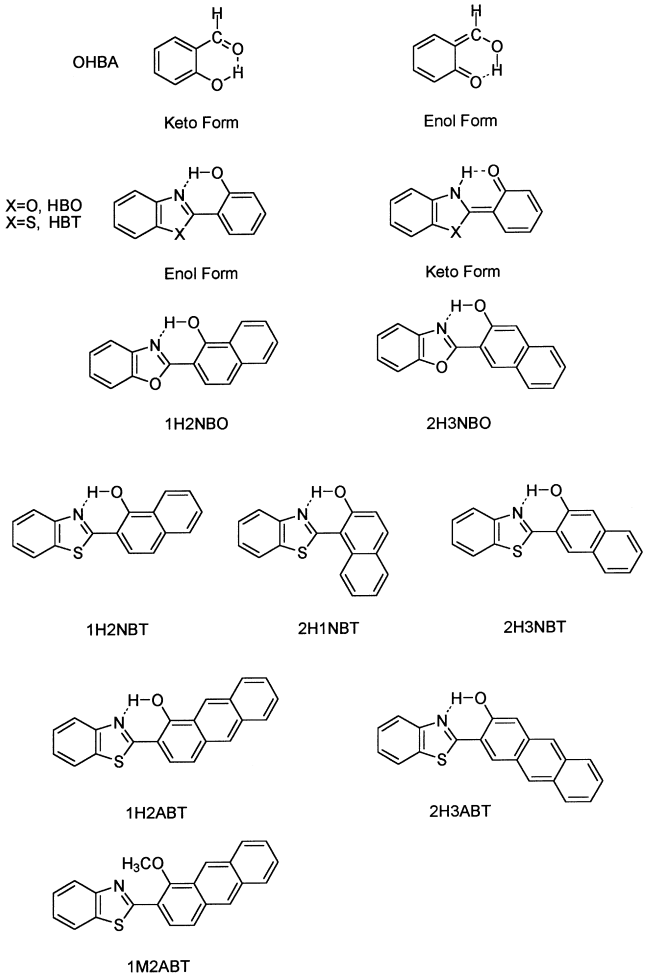

Fig. 1. Structure of molecules studied in the present work.

2. Nodal-plane model of ESIPT

The understanding of the mechanism of ESIPT in a simple molecule can lead to valuable insights into the behavior of complex systems. OHBA is the simplest example of an aromatic molecule with an intramolecular hydrogen bond, and it can exist in two tautomeric forms, the keto form and the enol form (proton-transferred form). The relative stability of each form depends on the electronic state of the molecule (Fig. 2): in the ground state (S_0 state), the keto form is stable, in the first excited $^1(\pi,\pi^*)$ state ($S_1^{(\pi)}$ state), ESIPT takes place to yield the enol form, and in the second excited $^1(\pi,\pi^*)$ state ($S_2^{(\pi)}$ state) the keto form is again stable.

The equilibrium constant between the enol forms of acetylacetaldehyde, $CH_3C(OH)=CHCHO$ (A form) and $CH_3COCH=CHOH$ (B form), was determined with NMR [58,59]. The broken curve in Fig. 3 (double-minimum potential) shows the potential curve of the two forms. The enol forms of malonaldehyde [HC(OH)=CHCHO] can also be characterized by a double-minimum potential [60–65]. Substitution of phenyl rings for the CH_3CCH

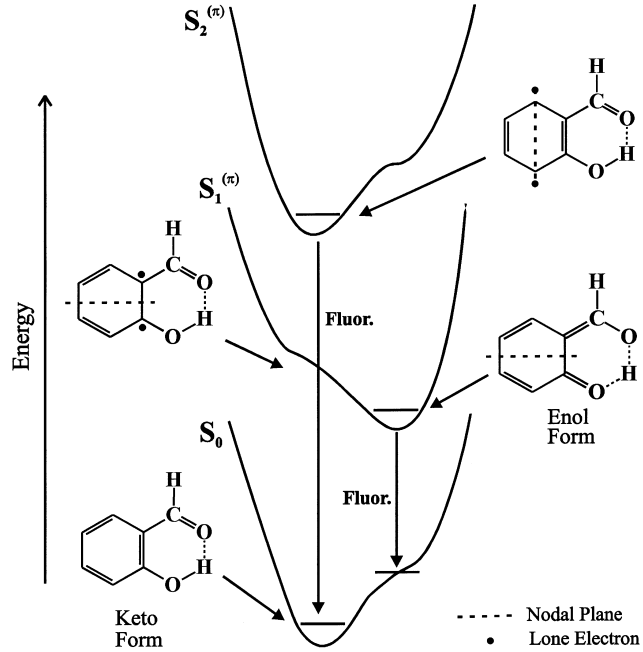

Fig. 2. Schematic representation of S_0, $S_1^{(\pi)}$ and $S_2^{(\pi)}$ potential surfaces for OHBA. Fluor. denotes fluorescence. The broken lines indicate the nodal planes perpendicular to the molecular plane, and the dots indicate seeming lone π electrons.

moieties in the acetylacetaldehyde enols, respectively, transforms the A and B forms into the keto and enol forms of OHBA (Fig. 3). The substitution stabilizes the A form owing to resonance of the phenyl ring [66], and the keto form of

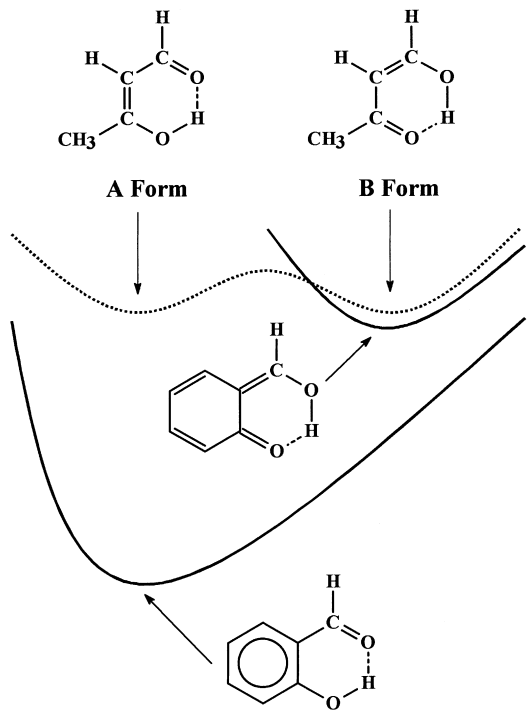

Fig. 3. Potential curves of acetylacetaldehyde enols (broken curve) [58,59] and OHBA (continuous curve).

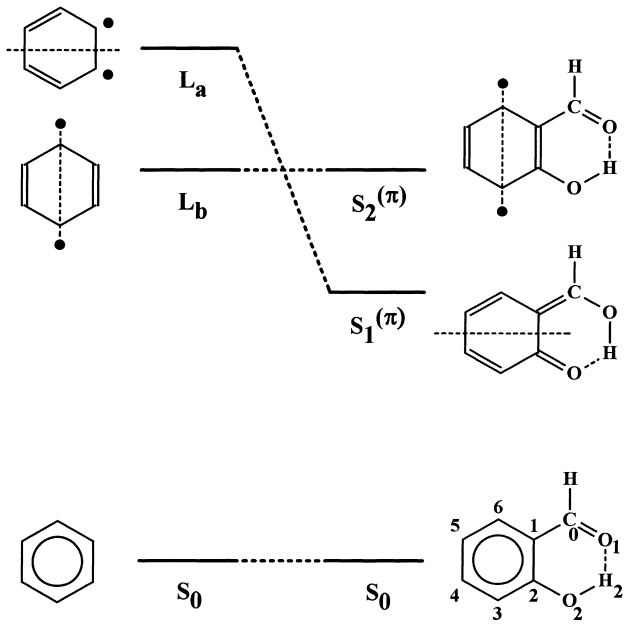

Fig. 4. Nodal planes of wave functions in several $^1(\pi,\pi^*)$ states of benzene and OHBA, and the numbering system for the atoms. The broken lines indicate the nodal planes perpendicular to the molecular plane, and the dots indicate seeming lone π electrons. Only one of the three positions of the nodal plane in the excited state of benzene is shown.

OHBA becomes markedly lower in energy than the A form of acetylacetaldehyde. The B form, in contrast, is not stabilized by the substitution, and the energy remains essentially unchanged on going from the B form to the enol form of OHBA. The schematic sketch of the potential curves of OHBA thus obtained (continuous curves in Fig. 3) is quite similar to that expected from the experimental results [21,22] for the S_0 and $S_1^{(\pi)}$ states of OHBA (Fig. 2): the $S_1^{(\pi)}$ state is thought to be much more susceptible to ESIPT than the S_0 state. From Fig. 3, we suggest that the presence of the phenyl ring has a large influence on the potential curves of the S_0 and $S_1^{(\pi)}$ states of OHBA.

Fig. 4 shows the nodal planes of the wave functions in several states of benzene and OHBA. As in the case of a particle in a two-dimensional rectangular potential box [67], the wave function of the S_0 state has no nodal plane and the wave functions of the S_1 and S_2 states each have one nodal plane: the nodal planes of the wave functions of the S_1 and S_2 states are perpendicular to each other. The S_1 and S_2 states of benzene ($^1(\pi,\pi^*)$ states) in the usual notation are L_b and L_a, respectively [68]. The wave function of the L_b state has a nodal plane through the C_2 and C_6 symmetry axes of point group D_{6h}, and that of the L_a state has a nodal plane through the C_2' and C_6 axes. In this paper, the C_2 symmetry axis of point group D_{6h} is taken to be located through two facing carbon atoms of benzene according to custom. Substitution of CHO and OH groups for adjacent H atoms of benzene results in OHBA (Fig. 4).

In the L_a state, one can write two double bonds along the nodal plane because π electrons are distributed over the molecule except on the nodal plane. When the two double bonds are C_3=C_4 and C_5=C_6, lone (unpaired) π electrons are localized at the C_1 and C_2 atoms. If ESIPT yielding the enol form takes place in the L_a state of OHBA, the two lone electrons can be largely delocalized as a result of the formation of the C_1=C_0 and C_2=O_2 bonds. The lone electrons thus facilitate the rearrangement of bonds to produce the enol form. The L_a state of the enol form of OHBA thus becomes significantly lower in energy than the L_a state of benzene owing to the delocalization, and in OHBA, the L_a state results in the $S_1^{(\pi)}$ state (Fig. 4). The enol form is preferred because of the more favorable nodal pattern in the $S_1^{(\pi)}$ state of OHBA.

In contrast, the wave function in the L_b state of OHBA has a nodal plane perpendicular to that in the L_a state (Fig. 4). ESIPT yielding the enol form cannot take place in the L_b state because C_0=C_1 and C_2=O_2 double bonds cannot be formed, and if these double bonds were formed, the C_1 and C_2 atoms would become pentavalent. As a result, the potential energy of the L_b state remains essentially unchanged on going from benzene to OHBA, and the potential curve is not distorted much from that of the S_0 state in OHBA. In OHBA, the L_b state thus results in the $S_2^{(\pi)}$ state (Fig. 4).

For these reasons, the $S_2^{(\pi)}$ state of OHBA is thought to be far less susceptible to ESIPT than the $S_1^{(\pi)}$ state is. This explanation is consistent with the emission properties of OHBAs [21–29,33,35,36]. We are therefore, led to the conclusion that the enol form is stabilized in the $S_1^{(\pi)}$ state owing to the properties of the nodal plane of the wave function.

In terms of our nodal-plane model, ESIPT is described by the skeletal distortion of the aromatic ring instead of by the change in the O–H···O structure. The structural reorganization in ESIPT is not localized around the hydrogen bond but rather encompasses the molecular framework. The main effect of the change in electronic structure due to the $S_0 \rightarrow S_1^{(\pi)}$ excitation ((π,π^*) transition) is on the π-bonding framework of the aromatic ring moiety instead of the σ-bonding of the hydrogen-bonded moiety. The electron redistribution upon excitation results in changes in bond order and bond length between heavy atoms like C and O. The change in O–H···O structure is relatively small and is strongly influenced by the movement of heavy atoms. In any given case, proton transfer in response to changes of the electron redistribution on the heavy atoms may or may not occur.

In our view, whether or not would ESIPT occur easily in an intramolecularly hydrogen-bonded molecule can be predicted directly from the wave function itself: the aromatic skeleton responds to the formation of the node in the $S_1^{(\pi)}$ wave function. Our concept is simple and readily provides a qualitative guide useful for predicting the more stable form in a particular electronic state [25–27,32–38]. We can predict the stabilization due to the ESIPT of medium-size polyatomic molecules without performing extensive calculations.

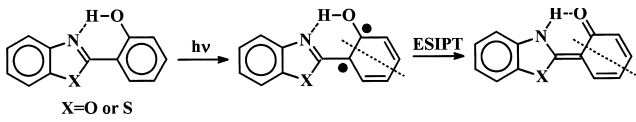

Scheme 1.

3. ESIPT of 2-(*o*-hydroxyaryl)benzazoles

The ESIPT of 2-(2-hydroxyphenyl)benzoxazole (HBO) and 2-(2-hydroxyphenyl)benzothiazole (HBT) has been studied extensively [30,31,69–74]. In the S_0 state, the enol form is stable, and in the $S_1^{(\pi)}$ state, ESIPT yields the keto form. As shown in Scheme 1, the mechanism of ESIPT in the $S_1^{(\pi)}$ states of HBO and HBT can be explained like that of the ESIPT in the $S_1^{(\pi)}$ state of OHBA. In this section, we will show the absorption and fluorescence spectra of 2-(*o*-hydroxynaphthyl)benzoxazoles, 2-(*o*-hydroxynaphthyl)benzothiazoles and 2-(*o*-hydroxyanthryl)benzothiazoles and will note that these experimental results strongly support our nodal-plane model.

3.1. Experimental methods

3.1.1. Sample preparation

2-(1-Hydroxy-2-naphthyl)benzoxazole (1H2NBO, Registry No. 32339-66-5) and 2-(2-hydroxy-3-naphthyl)benzoxazole (2H3NBO, Registry No. 14967-45-4) were prepared by condensation reactions, with polyphosphoric acid [75], between the corresponding hydroxynaphthoic acid and 2-aminophenol. 2-(1-Hydroxy-2-naphthyl)benzothiazole (1H2NBT, Registry No. 76995-70-5), 2-(2-hydroxy-1-naphthyl)benzothiazole (2H1NBT, novel compound) and 2-(2-hydroxy-3-naphthyl)benzothiazole (2H3NBT, Registry No. 25389-29-1) were prepared by condensation reactions, with phosphorus trichloride [76], between the corresponding hydroxynaphthoic acids and 2-aminothiophenol.

2H1NBT thus obtained was in the form of yellow needles, mp 119°C. ^{1}H NMR (270 MHz, $CDCl_3$, δ): 7.28 (d, $J = 8.9$ Hz, 1H), 7.34–40 (m, 2H), 7.49 (td, $J = 7.7$ and 1.3 Hz, 1H), 7.55–7.61 (m, 1H), 7.77–7.81 (m, 2H), 7.88 (d, $J = 7.3$ Hz, 1H), 7.99 (d, $J = 8.2$ Hz, 1H), 8.72 (d, $J = 8.5$ Hz, 1H), 14.21 (s, 1H, OH). Anal. Calcd. for $C_{17}H_{11}NOS$: C, 73.62; H, 4.00; N, 5.05. Found: C, 73.78; H, 4.23; N, 5.04.

In the preparation of 2-(1-hydroxy-2-anthryl)benzothiazole (1H2ABT, novel compound), 1-aminoanthracene was synthesized from 1-aminoanthraquinone [77], 1-anthrol was prepared from 1-aminoanthracene [77] and 1-anthrol-2-carboxylic acid was synthesized from 1-anthrol [78]. 1H2ABT was prepared by a condensation reaction, with phosphorus trichloride [76], between 1-anthrol-2-carboxylic acid and 2-aminothiophenol. It resulted in yellow plates, mp 265–266°C. ^{1}H NMR (400 MHz, $CDCl_3$ δ): 7.39–7.43 (m, 1H), 7.49–7.57 (m, 4H), 7.62 (d, $J = 8.8$ Hz, 1H), 7.94 (d, $J = 8.3$ Hz, 1H), 7.99–8.10 (m, 2H), 8.12 (d, $J = 7.8$ Hz, 1H), 8.35 (s, 1H), 9.12 (s, 1H), 14.21 (s, 1H, OH). Anal. Calcd. for $C_{21}H_{13}NOS$: C, 77.04; H, 4.00; N, 4.28. Found: C, 76.98; H, 4.28; N, 4.14.

In the present preparation of 2-(2-hydroxy-3-anthryl)benzothiazole (2H3ABT, Registry No. 116646-52-7), 4′-chloro-3′-methylbenzophenone-2-carboxylic acid was synthesized from phthalic anhydride and 2-chlorotoluene [79]. Then 2-chloroanthraquinone-3-carboxylic acid was synthesized from 4′-chloro-3′-methylbenzophenone-2-carboxylic acid [80], and 2-chloroanthracene-3-carboxylic acid was synthesized from 2-chloroanthraquinone-3-carboxylic acid [81]. After 2-hydroxyanthracene-3-carboxylic acid was prepared from 2-chloroanthracene-3-carboxylic acid [82,83], 2H3ABT was prepared by a condensation reaction, with phosphorus trichloride [76], between 2-hydroxyanthracene-3-carboxylic acid and 2-aminothiophenol. It resulted in yellow-orange grains, mp 277–278°C. ^{1}H NMR (400 MHz, $CDCl_3$ δ): 7.40–7.58 (m, 5H), 7.93–7.98 (m, 3H), 8.07 (d, $J = 7.8$ Hz, 1H), 8.26 (s, 1H), 8.48 (s, 1H), 8.54 (s, 1H), 12.15 (s, 1H, OH). Anal. Calcd. for $C_{21}H_{13}NOS$: C, 77.04; H, 4.00; N, 4.28. Found: C, 76.93; H, 4.20; N, 4.14.

2-(1-Methoxy-2-anthryl)benzothiazole (1M2ABT, novel compound) was synthesized from 1H2ABT and dimethyl sulfate by using a procedure similar to one reported previously [31,84]. It resulted in pale yellow needles, mp 224–225°C. ^{1}H NMR (400 MHz, $CDCl_3$ δ): 4.20 (s, 3H, CH_3), 7.41–7.45 (m, 1H), 7.51–7.57 (m, 3H), 7.91 (d, $J = 8.8$ Hz, 1H), 7.99–8.05 (m, 2H), 8.09–8.16 (m, 2H), 8.47 (s, 1H), 8.54 (d, $J = 9.3$ Hz, 1H), 8.79 (s, 1H). Anal. Calcd. for $C_{22}H_{15}NOS$: C, 77.39; H, 4.42; N, 4.10. Found: C, 77.16; H, 4.51; N, 4.08.

Hexane and cyclohexane prepared especially for luminescence were obtained from Nacalai Tesque and were used without further purification. 3-Methylpentane obtained from Tokyo Kasei Kogyo was purified twice by column chromatography on silica gel. The addition of a small amount of water to the sample solution did not have a large influence on the absorption and fluorescence spectra. However, the fluorescence spectra obtained from samples in polar solvents were very different from those obtained from samples in nonpolar solvents, and in polar solvents, the fluorescence–excitation spectra often differed from the absorption spectra.

3.1.2. Measurements

Unless otherwise stated, experiments were made at room temperature using a 1 cm^2 quartz static cell. The absorption spectra were measured with a Shimadzu UV-2100S spectrophotometer.

The nanosecond transient absorption spectrum of 2H3ABT was measured with a Unisoku TSP-601 time-resolved spectrophotometer equipped with a dye laser (Unisoku TSP-611) pumped by a Nd : YAG laser (Continuum Surelite I, 355 nm). Coumarin 440 (Exciton) was used as the dye. The measurement was based on pulse-pump (dye laser) and cw probe (Xe lamp) as the excitation sources. The sample concentration used was about 10^{-4} M. Prior to the

measurement at room temperature, the sample solution was degassed by bubbling nitrogen gas through it.

The fluorescence spectra at wavelengths below 900 nm were measured with a Shimadzu RF-5000 spectrophotometer. A Hamamatsu R928-08 photomultiplier tube was used as the detector. An emission spectrophotometer based on the photon-counting method was used for measuring the fluorescence spectra at wavelengths between 900 and 1200 nm (the details of the emission spectrophotometer have been reported previously [33]). In this study, the emission monochromator (Nikon G-250) was equipped with a 600 grooves mm^{-1} grating blazed at 750 nm and a Hamamatsu R649 or R1767 photomultiplier tube was used as the detector. The sample concentrations used were about 10^{-5} M.

3.2. Results and discussion

Fig. 5 shows the absorption and fluorescence spectra of 2H3NBO and 1H2NBO in hexane, and the wavelengths of the fluorescence peaks of 1H2NBO are in satisfactory agreement with those reported previously [55]. Although both 2H3NBO and 1H2NBO consist of a naphthalene nucleus, a benzoxazol-2-yl group and an OH group (Fig. 1), the emission properties of the two molecules are very different. As in HBO, ESIPT takes place in 1H2NBO which shows a Stokes-shifted ESIPT fluorescence emission around 470 nm (Fig. 5(b)). The absorption spectrum of 1H2NBO agrees well with the fluorescence-excitation spectrum. Unlike 1H2NBO, 2H3NBO shows dual fluorescence (Fig. 5(a)) like 2-(2-hydroxy-3-naphthyl)benzimidazole [56]. The short-wavelength fluorescence of 2H3NBO (~450 nm) may be due to an open conformer with the hydroxyl group not hydrogen-bonded to the oxazole nitrogen [56]. The long-wavelength fluorescence (~670 nm) is assigned to the ESIPT fluorescence of 2H3NBO. The absorption spectrum of 2H3NBO agrees well with the ESIPT fluorescence-excitation spectrum. The Stokes shift of the ESIPT fluorescence of 2H3NBO is much larger than that of 1H2NBO. Similar results were also obtained for 2H3NBT, 1H2NBT and 2H1NBT in hexane: the Stokes shift of the long-wavelength fluorescence of 2H3NBT is much larger than those of the fluorescence emissions of 1H2NBT and 2H1NBT. Since the absorption coefficient (ε) and the shape of the $S_0 \rightarrow S_1^{(\pi)}$ absorption band of 2H3NBO are very different from those of 1H2NBO, the potential surface of the $S_1^{(\pi)}$ state of 2H3NBO is expected to be very different from that of 1H2NBO.

The difference in the Stokes shift of the ESIPT fluorescence between 2H3NBO and 1H2NBO can be explained in terms of our nodal-plane model (Fig. 6). If one writes a nodal plane of the wave function in the $S_1^{(\pi)}$ state of

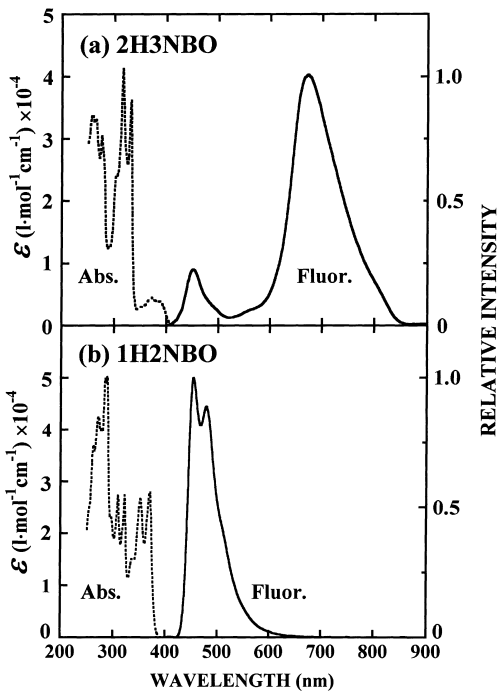

Fig. 5. Absorption (Abs.) and fluorescence (Fluor.) spectra of (a) 2H3NBO and (b) 1H2NBO in hexane. ε denotes the absorption coefficient. The fluorescence spectra have not been corrected for the spectral sensitivity of the detector. The fluorescence spectra of 2H3NBO and 1H2NBO were obtained by excitations at 330 and 350 nm, respectively.

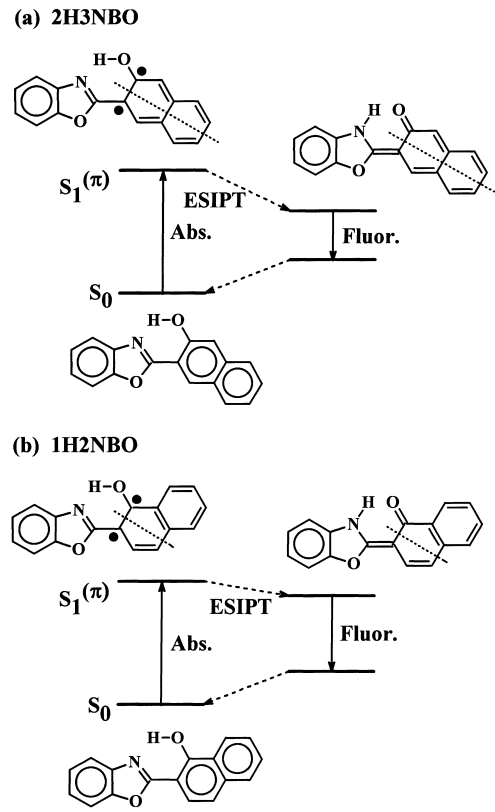

Fig. 6. Schematic energy-state diagram for dynamic processes in the S_0 and $S_1^{(\pi)}$ states of (a) 2H3NBO and (b) 1H2NBO in nonpolar solvents. The solid and broken arrows represent radiative and nonradiative processes, respectively. The broken lines indicate the nodal planes perpendicular to the molecular plane, and the dots indicate lone π electrons. Abs. and Fluor. denote absorption and fluorescence, respectively.

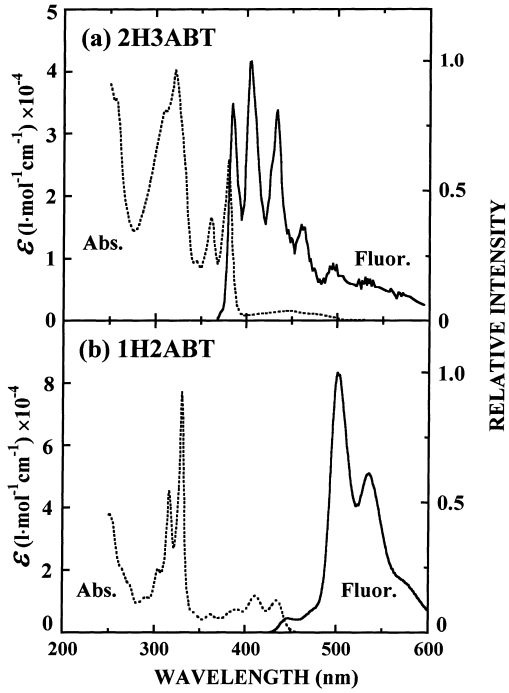

Fig. 7. Absorption (Abs.) and fluorescence (Fluor.) spectra of (a) 2H3ABT and (b) 1H2ABT in cyclohexane. ε denotes the absorption coefficient. The fluorescence spectra have not been corrected for the spectral sensitivity of the detector. The fluorescence spectra of 2H3ABT and 1H2ABT were obtained by excitations at 360 and 410 nm, respectively.

1H2NBO and the corresponding double bonds so as to get rid of lone π electrons, the nodal plane is localized on only one of the two six-membered rings in the naphthalene nucleus of the proton-transferred form (Fig. 6(b)). Such a proton-transferred form (keto form) is not expected to be very stable. In contrast, in the keto form of 2H3NBO, the wave function of the $S_1^{(\pi)}$ state has a nodal plane through both six-membered rings of the naphthalene nucleus (Fig. 6(a)). Thus the energy of the keto form of 2H3NBO is markedly lower than the energy of the keto form of 1H2NBO, and the Stokes shift of 2H3NBO is much larger than that of 1H2NBO. Furthermore, our nodal-plane model is also in accordance with the very recent report that methyl 2-hydroxy-3-naphthoate is the only methyl *o*-hydroxynaphthoate that exhibits an ESIPT emission [85].

Fig. 7 shows the absorption and fluorescence spectra of 2H3ABT and 1H2ABT in cyclohexane. Although 1M2ABT shows normal fluorescence, 1H2ABT shows a Stokes-shifted ESIPT fluorescence peak at 500 nm (Fig. 7(b)). This means that as in HBT, ESIPT takes place in 1H2ABT also. The absorption spectrum of 1H2ABT agrees well with the excitation spectrum obtained by monitoring the fluorescence at 500 nm. The weak fluorescence around 450 nm in 1H2ABT may originate from an open conformer with the hydroxyl group not hydrogen-bonded to the thiazole nitrogen. In contrast to 1H2ABT, 2H3ABT shows a fluorescence emission (Fig. 7(a)) blue-shifted even from that of 1M2ABT in which ESIPT never takes place. The fluorescence emission of 2H3ABT at long wavelengths (>700 nm) is negligible. The emission properties of 2H3ABT and 1H2ABT are thus very different even though both molecules consist of an anthracene moiety, a benzothiazol-2-yl group and an OH group (Fig. 1).

The $S_0 \rightarrow S_1^{(\pi)}$ absorption band of 2H3ABT is between 400 and 500 nm and the maximum value of ε is $1600\ \mathrm{l\ mol^{-1}\ cm^{-1}}$ at 450 nm. The 0–0 band of the $S_0 \rightarrow S_2^{(\pi)}$ excitation is at 380 nm where ε is $25\,900\ \mathrm{l\ mol^{-1}\ cm^{-1}}$. The emission spectrum of 2H3ABT shown in Fig. 7(a) was obtained upon excitation at the $S_0 \rightarrow S_2^{(\pi)}$ absorption band. Its red shift from the $S_0 \rightarrow S_2^{(\pi)}$ absorption band is small. The main bands of the emission spectrum shown in Fig. 7(a) are at wavelengths between the $S_0 \rightarrow S_2^{(\pi)}$ and $S_0 \rightarrow S_1^{(\pi)}$ absorption bands. Its excitation spectrum agrees well with the $S_0 \rightarrow S_2^{(\pi)}$ absorption spectrum. The emission shown in Fig. 7(a) is therefore attributable to the emission originating from 2H3ABT and is considered to be due to the $S_2^{(\pi)} \rightarrow S_0$ fluorescence.

The intensity of the $S_2 \rightarrow S_0$ fluorescence is usually much less than that of the $S_1 \rightarrow S_0$ fluorescence [86]. Exceptions occur only in azulenes [87], thiones [88–93], carotenoids [94,95], OHBAs [23,25,33] and other systems which exhibit strong $S_2 \rightarrow S_0$ fluorescence. The $S_2^{(\pi)} \rightarrow S_0$ fluorescence of 2H3ABT is another example of anomalous emission from upper excited states (violation of Kasha's rule [96]). Although the $S_2^{(\pi)} \rightarrow S_0$ fluorescence of OHBAs can be observed only when samples are in the vapor phase [23,25,33], that of 2H3ABT can be observed even when the sample is in solution.

The present observation of the $S_2^{(\pi)} \rightarrow S_0$ fluorescence from 2H3ABT is in accordance with our nodal-plane model (Fig. 8(a)). As in 2H3NBO and 1H2NBO, the proton-transferred form (keto form) of 2H3ABT is much more stabilized than that of 1H2ABT. Accordingly, as shown in Fig. 8, the energy gap between the zero-point vibrational levels of the $S_2^{(\pi)}$ and $S_1^{(\pi)}$ states is much larger for 2H3ABT than it is for 1H2ABT. Under these circumstances, the $S_2^{(\pi)} \rightarrow S_1^{(\pi)}$ internal-conversion (IC) of 2H3ABT must be, according to the energy gap law [97], much slower than that of 1H2ABT. The intensity of the fluorescence emission from the $S_2^{(\pi)}$ state of 2H3ABT is thus greater than that of the fluorescence emission from the $S_2^{(\pi)}$ state of 1H2ABT.

The emission due to excitation at the $S_0 \rightarrow S_1^{(\pi)}$ absorption band of 2H3ABT is negligible. The weak $S_1^{(\pi)} \rightarrow S_0$ fluorescence of 2H3ABT may be located at wavelengths above 1200 nm, or the potential curves of the S_0 and $S_1^{(\pi)}$ states that cross each other may result in the negligible $S_1^{(\pi)} \rightarrow S_0$ fluorescence in 2H3ABT. The transient absorption by excitation at the $S_0 \rightarrow S_1^{(\pi)}$ absorption band of 2H3ABT in 3-methylpentane is negligible at room temperature and 77 K. Since the ε, the transition energy and the shapes of the $S_0 \rightarrow S_1^{(\pi)}$ absorption band of 2H3ABT are very different from those of 1H2ABT, the potential surface of the $S_1^{(\pi)}$ state of 2H3ABT is expected to be very different from that of 1H2ABT.

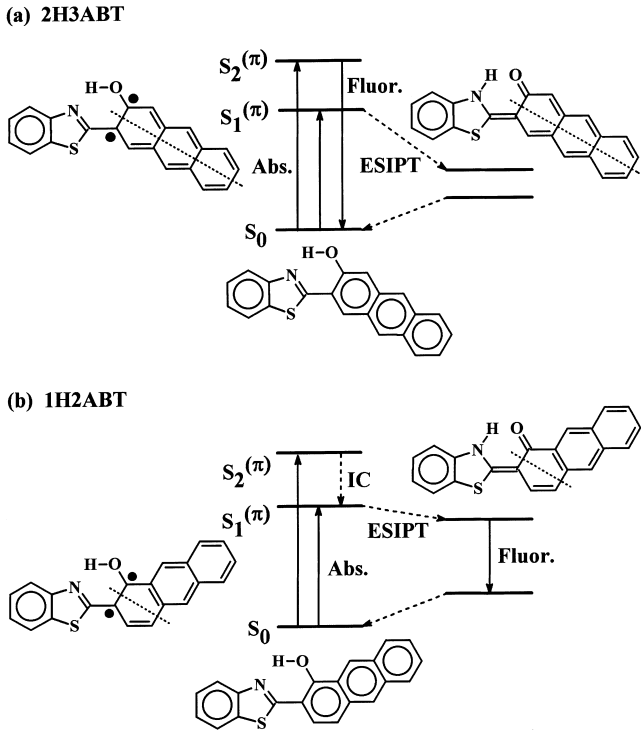

Fig. 8. Schematic energy-state diagram for dynamic processes in the S_0, $S_1^{(\pi)}$ and $S_2^{(\pi)}$ states of (a) 2H3ABT and (b) 1H2ABT in nonpolar solvents. The solid and broken arrows represent radiative and nonradiative processes, respectively. The broken lines indicate the nodal planes perpendicular to the molecular plane, and the dots indicate lone π electrons. Abs., Fluor. and IC denote absorption, fluorescence and internal-conversion, respectively. It should be noted in (b) that if one writes a nodal plane of the wave function in the $S_1^{(\pi)}$ state and the corresponding double bonds so as to get rid of lone π electrons, the nodal plane is localized on one of the three six-membered rings in the anthracene moiety of the keto form.

The Stokes shifts of the long-wavelength fluorescence of 2H3NBO and 2H3NBT (>10 000 cm^{-1}) are larger than those of the fluorescence of HBO and HBT (<8000 cm^{-1} [69,71,72]). Furthermore, although the $S_2^{(\pi)} \rightarrow S_0$ fluorescence emissions from 2H3NBO and 2H3NBT in solution are negligible, 2H3ABT shows a $S_2^{(\pi)} \rightarrow S_0$ fluorescence of moderate intensity (Fig. 7(a)), so the energy gap between the zero-point vibrational levels of the $S_2^{(\pi)}$ and $S_1^{(\pi)}$ states is likely to be much larger for 2H3ABT than for 2H3NBO or 2H3NBT. Thus when the nodal plane is oriented from one end of the aryl group to the other, the stabilization due to ESIPT is thought to increase with the number of six-membered rings condensed in the molecule. This view is reasonable because the delocalization of the lone electrons in the keto forms in Fig. 6(a) and Fig. 8(a) obviously increases with the number of six-membered rings.

4. Conclusions

The ESIPT of 2-(*o*-hydroxyaryl)benzazoles has been studied by emission spectroscopy. Although both 2-(2-hydroxy-3-aryl)benzazole and 2-(1-hydroxy-2-aryl)benzazole consist of an aryl moiety, a benzazol-2-yl group and an OH group, their emission properties are very different for reasons that can be explained in terms of our nodal-plane model [25,26]. Our nodal-plane model provides a simple but rather powerful concept for the understanding of ESIPT. Using it, we can predict the stabilization due to ESIPT of medium-size polyatomic molecules without performing extensive calculations.

Acknowledgements

We are indebted to Dr. Keishi Ohara and Mr. Arinobu Nakamura of Ehime University for their experimental support. We also thank Professor Satoshi Okazaki of Kyoto University and Professors Takashi Manabe and Hidenori Hayashi of Ehime University for their cooperation in the measurement of nanosecond transient absorption spectra. Shin-ichi Nagaoka expresses his sincere thanks to Professor Noboru Hirota of Kyoto University for his continuous encouragement. This work was partly supported by Grants-in-Aid for Scientific Research C (09640610) and for Scientific Research on Priority Area 'Quantum Tunneling of Group of Atoms as Systems with Many Degrees of Freedom' (Area 271/08240231, 09226229 and 10120225) from the Ministry of Education, Science, Sports and Culture of Japan.

References

[1] W. Klöffer, Adv. Photochem. 10 (1977) 311.
[2] P.M. Rentzepis, P.F. Barbara, Adv. Chem. Phys. 47(2) (1981) 627.
[3] D. Huppert, M. Gutman, K.J. Kaufmann, Adv. Chem. Phys. 47(2) (1981) 643.
[4] M. Kasha, J. Chem. Soc., Faraday Trans. II 82 (1986) 2379.
[5] P.F. Barbara, P.K. Walsh, L.E. Brus, J. Phys. Chem. 93 (1989) 29.
[6] P.F. Barbara, H.P. Trommsdorff, R.M. Hochstrasser, G.L. Hofacker (Eds.), Spectroscopy and Dynamics of Elementary Proton Transfer in Polyatomic Systems, Chem. Phys. 136 (1989) 153–360.
[7] M. Kasha Festschrift, in: P.F. Barbara, M. Nicol, M.A. El-Sayed (Eds.), J. Phys. Chem. 95 (1991) 10215–10524.
[8] S.J. Formosinho, L.G. Arnaut, J. Photochem. Photobiol. A 75 (1993) 21.
[9] H. Shizuka (Ed.), Proc. 54th Okazaki Conf. on Dynamic Studies on Hydrogen Atom Transfer Reactions, Institute for Molecular Science, Gunma University, Okazaki, Kiryu, 1996.
[10] A. Douhal, F. Lahmani, A.H. Zewail, Chem. Phys. 207 (1996) 477.
[11] G.A. Kraus, W. Zhang, M.J. Fehr, J.W. Petrich, Y. Wannemuehler, S. Carpenter, Chem. Rev. 96 (1996) 523.
[12] R.C. Haddon, F.H. Stillinger, in: F.L. Carter (Ed.), Molecular Electronic Devices, Ch II, Marcel Dekker, New York, USA, 1982.
[13] H. Sixl, D. Higelin, in: F.L. Carter (Ed.), Molecular Electronic Devices II, Part I–2, Marcel Dekker, New York, USA, 1987.
[14] M.A. Ratner, J. Jortner, in: J. Jortner, M. Ratner (Eds.), Molecular Electronics, Ch 1, Blackwell Science, Oxford, UK, 1997.
[15] A. Sytnik, M. Kasha, Proc. Natl. Acad. Sci. USA 91 (1994) 8627.
[16] A. Sytnik, D. Gormin, M. Kasha, Proc. Natl. Acad. Sci. USA 91 (1994) 11968.

[17] J. Keck, H.E.A. Kramer, H. Port, T. Hirsch, P. Fischer, G. Rytz, J. Phys. Chem. 100 (1996) 14468 and references cited therein.
[18] Shin Keshohin Gaku (New Cosmetic Science), section 5.5, T. Mitsui (Ed.), Nanzando, Tokyo, Japan, 1993.
[19] M. Kasha, in: F.L. Carter, R.E. Siatkowski, H. Wohltjen (Eds.), Molecular Electronic Devices, North-Holland, Amsterdam, 1988, pp. 107–121.
[20] A. Sytnik, M. Kasha, Radiat. Phys. Chem. 41 (1993) 331.
[21] S. Nagaoka, N. Hirota, M. Sumitani, K. Yoshihara, J. Am. Chem. Soc. 105 (1983) 4220.
[22] S. Nagaoka, N. Hirota, M. Sumitani, K. Yoshihara, E. Lipczynska-Kochany, H. Iwamura, J. Am. Chem. Soc. 106 (1984) 6913.
[23] S. Nagaoka, M. Fujita, T. Takemura, H. Baba, Chem. Phys. Lett. 123 (1986) 489.
[24] S. Nagaoka, J. Photochem. Photobiol. A 40 (1987) 185.
[25] S. Nagaoka, U. Nagashima, N. Ohta, M. Fujita, T. Takemura, J. Phys. Chem. 92 (1988) 166.
[26] S. Nagaoka, U. Nagashima, Chem. Phys. 136 (1989) 153.
[27] S. Nagaoka, Chem. Chem. Ind. 44 (1991) 182.
[28] U. Nagashima, S. Nagaoka, S. Katsumata, J. Phys. Chem. 95 (1991) 3532.
[29] E. Hoshimoto, S. Yamauchi, N. Hirota, S. Nagaoka, J. Phys. Chem. 95 (1991) 10229.
[30] S. Nagaoka, A. Itoh, K. Mukai, E. Hoshimoto, N. Hirota, Chem. Phys. Lett. 192 (1992) 532.
[31] S. Nagaoka, A. Itoh, K. Mukai, U. Nagashima, J. Phys. Chem. 97 (1993) 11385.
[32] S. Nagaoka, U. Nagashima, Chem. Phys. 206 (1996) 353.
[33] S. Nagaoka, Y. Shinde, K. Mukai, U. Nagashima, J. Phys. Chem. A 101 (1997) 3061.
[34] S. Nagaoka, S. Yamamoto, K. Mukai, J. Photochem. Photobiol. A 105 (1997) 29.
[35] S. Nagaoka, U. Nagashima, Trends Phys. Chem. 6 (1997) 55.
[36] S. Nagaoka, U. Nagashima, Photochem. 28 (1998) 39.
[37] S. Nagaoka, U. Nagashima, J. Phys. Chem. 94 (1990) 1425.
[38] S. Nagaoka, U. Nagashima, J. Phys. Chem. 95 (1991) 4006.
[39] A. Grabowska, A. Mordziñski, N. Tamai, K. Yoshihara, Chem. Phys. Lett. 153 (1988) 389.
[40] J.L. Herek, S. Pedersen, L. Bañares, A.H. Zewail, J. Chem. Phys. 97 (1992) 9046.
[41] A. Grabowska, J. Sepioł, C. Rullière, J. Phys. Chem. 95 (1991) 10493.
[42] A.L. Sobolewski, W. Domcke, Chem. Phys. 184 (1994) 115.
[43] M.V. Vener, S. Scheiner, J. Phys. Chem. 99 (1995) 642.
[44] P.B. Bisht, H. Petek, K. Yoshihara, U. Nagashima, J. Chem. Phys. 103 (1995) 5290.
[45] A.L. Sobolewski, W. Domcke, in: D. Heidrich (Ed.), The Reaction Path in Chemistry: Current Approaches and Perspectives, Kluwer Academic Publishers, Amsterdam, 1995, pp. 257–282.
[46] M.P. Marzocchi, A.R. Mantini, M. Casu, G. Smulevich, J. Chem. Phys. 108 (1998) 534.
[47] A.L. Sobolewski, W. Domcke, Chem. Phys. 232 (1998) 257.
[48] S. Tobita, M. Yamamoto, N. Kurahayashi, R. Tsukagoshi, Y. Nakamura, H. Shizuka, J. Phys. Chem. A 102 (1998) 5206.
[49] S. Takeuchi, T. Tahara, J. Phys. Chem. A 102 (1998) 7740.
[50] A. Graneß, H. Hartmann, J. Kleinschmidt, Z. Phys. Chem. (Leipzig) 261 (1980) 946.
[51] A. Graneß, J. Kleinschmidt, Z. Phys. Chem. (Leipzig) 261 (1980) 1152.
[52] J. Kleinschmidt, A. Graness, J. Photochem. 22 (1983) 33.
[53] G.F. Kirkbright, D.E.M. Spillane, K. Anthony, R.G. Brown, J.D. Hepworth, K.W. Hodgson, Anal. Chem. 56 (1984) 1644.
[54] K. Anthony, R.G. Brown, J.D. Hepworth, K.W. Hodgson, B. May, M.A. West, J. Chem. Soc., Perkin Trans. 2 (1984) 2111.
[55] A. Graneß, G. Graneß, Z. Phys. Chem. (Leipzig) 267 (1986) 173.
[56] A. Douhal, F. Amat-Guerri, A.U. Acuña, K. Yoshihara, Chem. Phys. Lett. 217 (1994) 619.
[57] S. Nagaoka, J. Kusunoki, A. Nakamura, T. Fujibuchi, K. Mukai, Book of Abstracts, in: 17th IUPAC Symp. on Photochemistry, Sitges, Barcelona, Spain, 19–24 July 1998, PA-2.
[58] J. Castells, J. Soler, An. Quim. 72 (1976) 1037.
[59] J. Castells, J. Soler, Chem. Abstr. 87(25) (1977) 200661z.
[60] W.F. Rowe, R.W. Duerst, E.B. Wilson, J. Am. Chem. Soc. 98 (1976) 4021.
[61] P. Turner, S.L. Baughcum, S.L. Coy, Z. Smith, J. Am. Chem. Soc. 106 (1984) 2265.
[62] D.W. Firth, P.F. Barbara, H.P. Trommsdorff, Chem. Phys. 136 (1989) 349 and references cited therein.
[63] N. Shida, P.F. Barbara, J.E. Almlöf, J. Chem. Phys. 91 (1989) 4061.
[64] T. Chiavassa, P. Roubin, L. Pizzala, P. Verlaque, A. Allouche, F. Marinelli, J. Phys. Chem. 96 (1992) 10659 and references cited therein.
[65] T.D. Sewell, Y. Guo, D.L. Thompson, J. Chem. Phys. 103 (1995) 8557 and references cited therein.
[66] G. Herzberg, Molecular Spectra and Molecular Structure III Electronic Spectra and Electronic Structure of Polyatomic Molecules, Ch III, Van Nostrand Reinhold, New York, USA, 1966.
[67] P.W. Atkins, Physical Chemistry, 5th ed., Freeman, New York, USA, 1994, pp. 398–400.
[68] J.B. Birks, in: J.B. Birks (Ed.), Organic Molecular Photophysics, vol. 1, Ch 1, Wiley, London, UK, 1973.
[69] P.F. Barbara, L.E. Brus, P.M. Rentzepis, J. Am. Chem. Soc. 102 (1980) 5631.
[70] T. Elsaesser, W. Kaiser, Chem. Phys. Lett. 128 (1986) 231.
[71] M.F. Rodríguez Prieto, B. Nickel, K.H. Grellmann, A. Mordziñski, Chem. Phys. Lett. 146 (1988) 387.
[72] K.H. Grellmann, A. Mordziñski, A. Heinrich, Chem. Phys. 136 (1989) 201.
[73] W. Al-Soufi, K.H. Grellmann, B. Nickel, J. Phys. Chem. 95 (1991) 10503.
[74] H. Eisenberger, B. Nickel, A.A. Ruth, W. Al-Soufi, K.H. Grellmann, M. Novo, J. Phys. Chem. 95 (1991) 10509.
[75] C.M. Orlando Jr., J.G. Wirth, D.R. Heath, J. Org. Chem. 35 (1970) 3147.
[76] D.L. Williams, A. Heller, J. Phys. Chem. 74 (1970) 4473.
[77] H.E. Fierz-David, L. Blangey, H. Streiff, Helv. Chim. Acta 29 (1946) 1718.
[78] S.S. Lele, N.H. Shah, S. Sethna, J. Org. Chem. 21 (1956) 1293.
[79] Gesellschaft für Chemische Industrie, Basel, Ger. Patent (1908) 205218.
[80] K. Schirmacher, K. Billing, I.G. Farbenindustrie Akt.-Ges., Frankfurt, Ger. Patent (1932) 556161.
[81] L. Sander, S. Gassner, I.G. Farbenindustrie Akt.-Ges., Frankfurt, Ger. Patent (1932) 547352.
[82] V.N. Lisitsyn, G.G. Bakulina, T.V. Sedova, N.N. Vorozhtsov Jr., J. Gen. Chem. USSR (Engl. Transl.) 32 (1962) 3661.
[83] V.N. Lisitsyn, G.G. Bakulina, T.V. Sedova, N.N. Vorozhtsov Jr., Zh. Obshch. Khim. 32 (1962) 3734.
[84] R. Nakagaki, T. Kobayashi, S. Nagakura, Bull. Chem. Soc. Jpn. 51 (1978) 1671.
[85] J. Catalán, J.C. del Valle, J. Palomar, P. Pérez, C. Díaz, J.L.G. de Paz, Book of Abstracts, in: 17th IUPAC Symp. on Photochemistry, Sitges, Barcelona, Spain, 19–24 July 1998, PA-87.
[86] J.B. Birks, in: J.B. Birks (Ed.), Organic Molecular Photophysics, vol. 2, Ch 9, Wiley, London, UK, 1975.
[87] M. Beer, H.C. Longuet-Higgins, J. Chem. Phys. 23 (1955) 1390.
[88] M. Mahaney, J.R. Huber, Chem. Phys. 9 (1975) 371.
[89] T. Oka, A.R. Knight, R.P. Steer, J. Chem. Phys. 66 (1977) 699.
[90] M. Mahaney, J.R. Huber, Chem. Phys. Lett. 105 (1984) 395 and references cited therein.
[91] N. Boens, M. van den Zegel, F.C. de Schryver, Chem. Phys. Lett. 111 (1984) 340.
[92] K.J. Falk, A.R. Knight, A. Maciejewski, R.P. Steer, J. Am. Chem. Soc. 106 (1984) 8292 and references cited therein.

[93] A. Maciejewski, D.R. Demmer, D.R. James, A. Safarzadeh-Amiri, R.E. Verrall, R.P. Steer, J. Am. Chem. Soc. 107 (1985) 2831.
[94] M. Mimuro, U. Nagashima, S. Nagaoka, Y. Nishimura, S. Takaichi, T. Katoh, I. Yamazaki, Chem. Phys. Lett. 191 (1992) 219.
[95] M. Mimuro, Y. Nishimura, S. Takaichi, Y. Yamano, M. Ito, S. Nagaoka, I. Yamazaki, T. Katoh, U. Nagashima, Chem. Phys. Lett. 213 (1993) 576.
[96] M. Kasha, Discuss. Faraday Soc. 9 (1950) 14.
[97] R. Englman, J. Jortner, Mol. Phys. 18 (1970) 145.